Computational Simulation for Cylinder Vibration under Interference of a Stationary Cylinder

Zhendong Cui[1,2,3], Zhengshou Chen[3,4]

1 *School of Mathematics*, Physics & Information Science, Zhejiang Ocean University, Zhoushan, Zhejiang 316022, P. R. China
2 Key Laboratory of Oceanographic Big Data Mining & Application of Zhejiang Province, Zhoushan, 316022, P. R. China
3 Key Laboratory of Offshore Engineering Technology of Zhejiang Province, Zhoushan, Zhejiang 316022, P. R. China
4. Zhejiang Ouhua Shipbuilding Co., Ltd, Zhoushan, Zhejiang 316000, P. R. China
*Tel. +86 580 2550029, e-mail: cuizhendong@126.com

***Abstract* — One degree of freedom vibration in cross-flow direction of an elastically mounted cylinder was simulated numerically in the wake of a stationary cylinder. The mass ratio was 1.9, and the spacing ratios of 5. The reduced velocities range from 2 to 16.5 with an interval of 0.5. Four regimes are found in the response of the cylinder under the interference of the upstream stationary cylinder. The numerical results indicate the vortexes from the upstream cylinder will take significant impact on cross-flow vibration of the downstream cylinder in the regime 2 of 5≤Vr≤8.5. Outside this range, the effect from the upstream stationary cylinder is week. The vibration of the downstream cylinder is something like the isolated cylinder.**

Keywords-Vortex Shedding, Vortex Induced Vibration

I. INTRODUCTION

Vortex shedding from a bluff body has been extensively investigated in the past decades for its close relevance to the engineering applications and its characteristic as a fundamental fluid mechanic. The wake of a stationary circular cylinder in steady flow consists of two staggered rows of vortex when the Reynolds numbers exceeds about 40. The vortices shedding leads to aperiodic force exerting on the cylinder, which generate the lift force having the same frequency as the vortex shedding cycle, and the frequency of drag equaling twice of the shedding frequency. Vortex shedding will be dramatically changed when the cylinder oscillates in flow stream, not only in the cross flow direction but also in the flow direction. Bishop and Hassan(1964)[1] investigated experimentally the hydrodynamic forces exerted on the cylinder in the cross-flow direction, and found that significant changed of the mean drag and the lift amplitude when the excitation frequency is close to the natural shedding frequency. Feng(1968)[2] studied VIV of a cylinder in the cross-flow direction at high mass ratio and found that the resonance of the vibration occurred at a range of reduced velocity. The resonance is also called lock-in because the vibration frequency of the cylinder is locked onto the natural frequency instead of following the Strouhal law. The response regime of the reduced velocity was classified into an initial branch, where the response amplitude increases with the increasing reduced velocity and a lower branch where the response amplitude decreases with the increasing reduced velocity.

It has been well understood that the flow regimes in the wake of a circular cylinder depend greatly on the Reynolds number defined by Re = Ud/ν, where d is the diameter the cylinder, U the flow velocity and ν is the kinematic viscosity. Comprehensively reviews of flow past cylinders can be found in Bearman(1984)[3], Williamson(1996)[4], Sumer and Fredsøe(1997)[5] and Williamson and Govardhan (2004)[6].

Both flow past two stationary cylinders and VIV of two identical cylinders have been studied extensively. Flow induced vibration of two identical cylinders have also been studied extensively. Zdravkovich (1985)[7] found that the oscillation amplitude depends very strongly on the relative locations of the two cylinders. When the distance of two identical stationary cylinders with tandem arrangement is not more than the critical distance, the vortex shedding is found to occur only from the downstream cylinder (Meneghini et al., 2001[8]; Mizushima and Suehiro, 2005[9]; Tasaka et al., 2006[10]). The critical distance is between 3.0-3.5 cylinder diameters, which depends on the Reynolds number. Assi(2006)[11] investigated experimentally the flow-induced oscillations of circular cylinders arranged in tandem in the region of reduced velocity less than 10. Cui(2014)[12] studied the vortex-induced vibration of two elastically coupled cylinders in side-by-side arrangement, and found that the elastically coupling took a great effects on the vibration.

One degree of freedom (1-dof) vibration in cross-flow direction of an elastically mounted cylinder was simulated numerically in the wake of a stationary cylinder, which the upstream cylinder is maintained fixed. The structure of the paper is arranged as follows. The numerical model is briefly described in the next section followed some numerical verifications and validations. The numerical results are presented in Section 3, focusing on the displacement and lift of the downstream cylinder. Finally, conclusions are drawn in Section 4.

II.COMPUTATIONAL MODEL

A. Numerical method

The two-dimensional numerical models are employed to simulate the 1-dof vibration of the cylinder in this paper. The governing equations for simulating the flow are the two-dimensional incompressible Navier-Stokes (N-S) equations. The Arbitrary Lagrangian Eulerian (ALE) scheme is applied to treat moving boundaries of the cylinder surfaces, which allows the boundaries of the computational mesh to move with the cylinders. In this study the reduced velocity u_i (i=1,2), the time t, the length (x, y) and the pressure p are nondimensionalized by

$$x_i = \tilde{x}_i / d,\ u_i = \tilde{u}_i / (f_n d),\ t = \tilde{t} f_n,\ p = \tilde{p} / (\rho f_n^2 d^2), \quad (1)$$

where the tilde denotes the dimensional parameters, $x_1=x$ and $x_2=y$ are the Cartesian coordinates, $\tilde{u}_1 = V_r$ is the inline velocity and $\tilde{u}_2$ is the cross-flow velocity, ρ is the fluid density, f_n is the natural vibration frequency, and d is the diameter of the cylinder. The non-dimensional ALE formulation of the RANS equations for incompressible flows are expressed as

$$\frac{\partial u_i}{\partial x_i} = 0, \quad (2)$$

$$\frac{\partial u_i}{\partial t} + \left(u_j - \hat{u}_j\right)\frac{\partial u_i}{\partial x_j} = -\frac{\partial p}{\partial x_i} + \frac{V_r}{\mathrm{Re}}\frac{\partial^2 u_i}{\partial x_i^2} + \frac{\partial}{\partial x_j}\left(-\overline{u_i' u_j'}\right), \quad (3)$$

where $\hat{u}_i$ is the velocity of the mesh movement in the xi-direction, Re is the Reynolds number. The Reynolds stress tensor $\overline{u_i' u_j'}$ is computed by

$$-\overline{u_i' u_j'} = \nu_t(\partial u_i / \partial x_j + \partial u_j / \partial x_i) + \frac{2}{3} k\delta_{ij}, \quad (4)$$

where ν_t is the turbulent viscosity and k is the turbulent energy. The shear stress transport (SST) k-ω turbulence model is used for modelling the turbulence. The detail of the turbulence model can be found in Menter (1994)[13]. The boundary conditions for the governing equations need to be given for solving the RANS equations. At the surfaces of the cylinders, the no-slip boundary condition is employed, i.e. the fluid velocity on each cylinder surface is the same as the vibrating speed of the cylinder. At the cylinder surfaces, the turbulent energy k is zero and the specific dissipation rate ω is given at the nodal points next to the wall surface as $\omega = 6\,\mathrm{Re}/\Delta_1^2$, where Δ_1 is the distance from the wall. The inlet velocity boundary conditions are set as $u = V_r$, $v = 0$. The nondimensional turbulence quantities are $k = 0.001 V_r^2$ and $\omega = 1$ (Guilmineau and Queutey, 2004)[14]. At the outflow boundary, the gradients of fluid velocity and turbulent quantities in the direction normal to the boundary are set to be zero. Pressure at the outflow boundary is given a reference value of zero (Pan et al., 2007)[15]. After each computational time step, the positions of the cylinders are changed and the computational mesh needs to be updated accordingly.

The motion of the cylinder is predicted by solving the equation of the motion

$$\frac{\mathrm{d}^2 X}{dt^2} + C\frac{\mathrm{d}X}{\partial t} + KX = F, \quad (5)$$

where X is the displacements of the cylinder in the x-directions, C and K are damping and spring constants, respectively, F is the forces on the small cylinder in the x-direction. The N-S equations are solved by the Petrov-Galerkin finite element method (PG-FEM) by Zhao et al. (2007)[16].

The governing equation for calculating the displacements of the nodes of the FEM mesh is (Zhao and Cheng, 2011)[17]

$$\nabla \cdot \left(\gamma \nabla \Delta_i\right) = 0, \text{ (i=1,2)}, \quad (6)$$

where Δ_i represents the displacement of the nodal points in the x_i -direction, and γ is a parameter that controls the mesh deformation. To avoid excessive deformation of the near-wall elements, the parameter γ in an finite element is set to be $\gamma = 1/A$, with A being the area of the element. The displacement of the mesh nodes is the same as the displacement of the cylinder on the cylinder surface and zero on other boundaries. By giving the displacements at all the boundaries, Eq. (6) is solved by a Galerkin FEM. Initially, the velocity and the pressure are zero in the whole computational domain and the cylinder's displacement and velocity are zero in all the simulations.

B. Configuration and computational mesh

A pair of cylinders in tandem arrangement with same diameter d has been considered that is shown in Fig.1. The upstream cylinder is stationary, and the downstream cylinder is elastically mounted that can freely vibrate in the cross-flow direction.

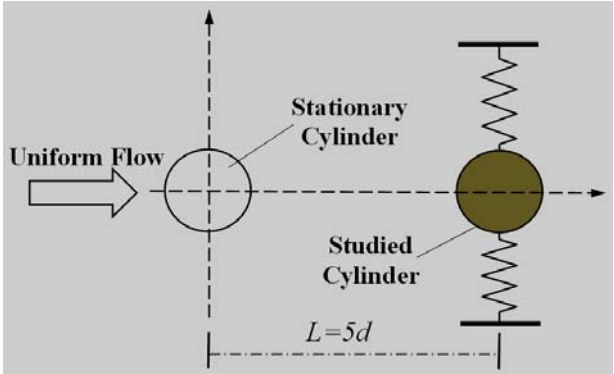

Fig.1 Sketch of two circular cylinders in tandem

The mass ratio was 1.9, the distance is 5d, and the damping ratio is 0.013 which is very close to the experiment parameters of Assi et al. (2006)[11]. A rectangular computational domain was adapted with a height of 45d in the cross-flow direction and a width of 40d in the flow direction is used. The distance between the inlet boundary and the center of the stationary cylinder is 20d. The numerical simulations are carried out by the two-dimensional numerical model described in Section 2.1. The circumference of each cylinder is discretized by 160 nodes and the total finite element node number is 53,399. The minimum mesh size at the cylinder surface in the radial direction is 0.00025d. In order to validate the computational method and find the more vibration law, the U/Re was kept to a constant value in this study which is the same condition in the experiment, and the reduced velocities ranges from 2.5 to 20 with an interval of 0.5.

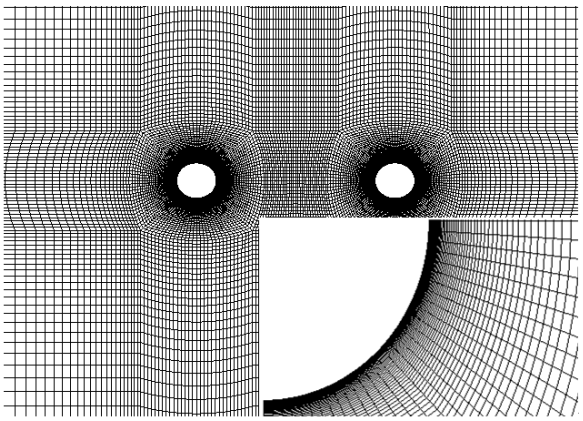

Fig.2 Local mesh near the cylinder

III.NUMERICAL RESULTS

A. Vibration amplitude and frequency

The amplitude of the elastically mounted cylinder 1 in the downstream is presented in Fig.3, which is defined as Ay=(Ymax-Ymin)/2. The Ymax and Ymin are the maximum and the minimum displacements of a cylinder in at least 100 periods of vibration.

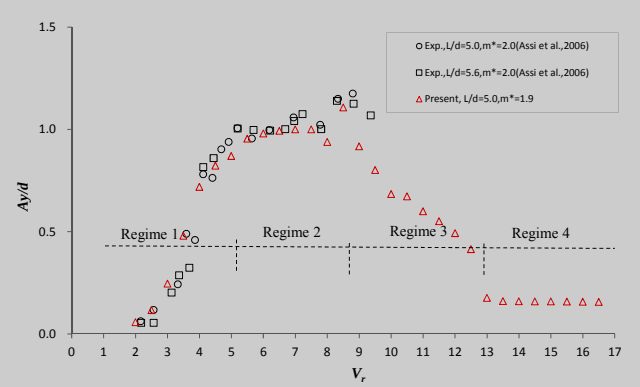

Fig.3 Variation of the reduced amplitude Ay/d versus reduced velocity Vr for the downstream cylinder

The experiment results by Assi et al(2006)[11] are also drawn in the figure in order to validate the numerical method. The numerical results and the experiment data takes on a good agreement in Fig.3, which prove the numerical method having a high accuracy in simulating the problem.

The oscillation starts at about Vr=2 and grow continuously when Vr<8.5. Between the 8.5< Vr <12.5, the amplitude of the downstream cylinder takes on a linear decreasing with the increasing of reduced velocity. When the Vr >12.5, the amplitude of the downstream cylinder becomes very small and keep an almost constant value with the increasing of the reduced velocity.

Fig.4 presents the variation of vibration frequencies with reduced velocity. For an isolated elastically mounted cylinder, Bearman(1984)[3] found the vibrating frequency locks onto the natural frequency in the resonance at high mass ration, and Govardhan and Williamson(2000)[18] proved the response frequency will be significantly higher than the natural frequency if the mass ratio is in the order 0(1). It can be seen from the Fig.4, the vibrating frequency of the downstream locks onto the natural frequency when 8.5<Vr≤ 12.5, and is very close to the natural frequency when 5<Vr≤ 8.5. In the regime of Vr≤ 5, the vibration frequency increases with the reduced velocity in a linear variation, and a similar phenomenon will occurs when the reduced velocity exceeds 12.5.

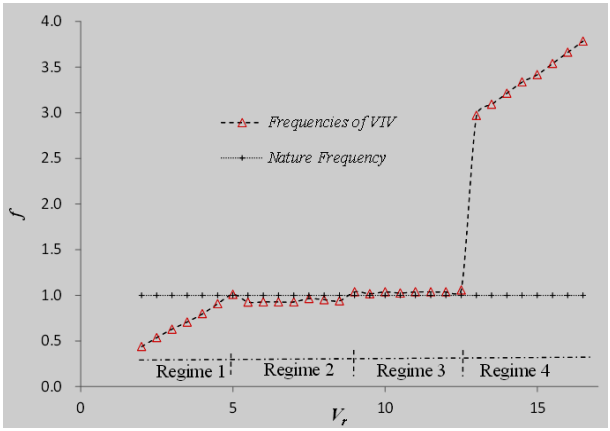

Fig.4 Vibration Frequencies of downstream cylinder of the two cylinders in tandem

Based on the varying of amplitudes and frequencies versus reduced velocities, fours regimes are divided for the vibration response of the downstream cylinder in the tandem arrangement. When the Vr≤ 5, this range is defines regime1. In the regime 1, both the amplitudes and frequencies of the cylinder increases with the growing of the reduced velocities, and the vibration of the cylinder is regular. When the reduced velocities between the 5 and 8.5, the vibration of the cylinder become irregularly, and the frequencies is about 0.95 which is very close to the cylinder natural frequencies. What is more, the amplitudes in the regime stay in a high value with the peak of 1.1. This region called the regime 2. The range of 8.5<Vr≤ 12.5 is defined regime 3, in which the vibration frequencies keep to natural frequency of the cylinder, and the vibration amplitudes decrease with the increasing of the reduced velocities in a linear manner. When the reduced velocity exceeds 12.5, the amplitude of the cylinder becomes very small and the frequencies increase linearly with increasing of the reduced velocities. The amplitudes keep the value that is not greater than 0.16, and takes no obviously change with the varying of the reduced velocity. This range defined the regime 4 in the study.

Fig.5 presents displacement and lift force time history of the downstream cylinder for some representative reduced velocities. The FL is the lift acting on the elastically mounted cylinder in the downstream, which is defined as $FL=(F_{max}-F_{min})/(\rho U^2 D/2)$. The Fmax and Fmin are the maximum and the minimum lift force of the cylinder in at least 100 periods of vibration.

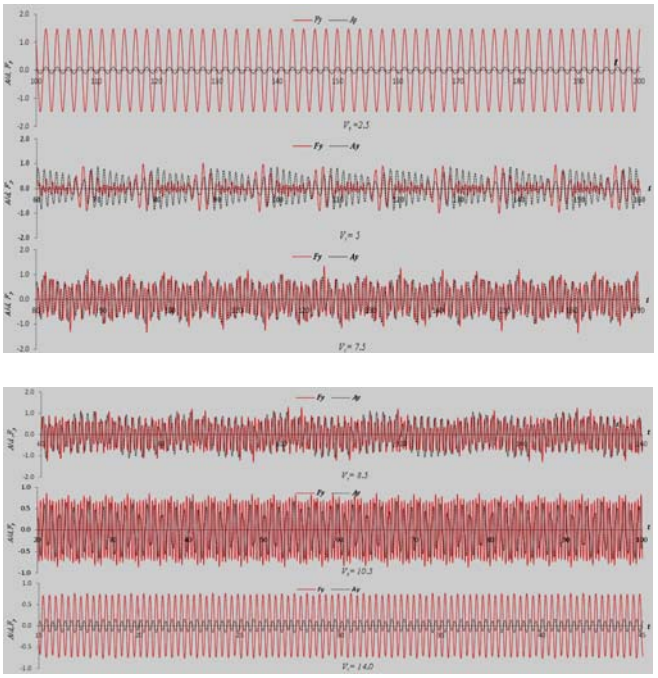

Fig.5 The displacement and lift time history of the downstream cylinder

The case of Vr=2.5 is in the regime 1 in this study. The time history of displacements and lift force change very regularly, and the phase of displacement and the lift force are closing to 180 degrees. The cases of Vr=5, 6.5, and 8.5 are in the regime2, which the vibration becomes irregular, and the phases of displacement and the lift force becomes unpredictable. The irregular displacement peaks lead to the amplitude of the vibration in a high value. When the reduced velocity is 10.5 in the regime 3, the vibration becomes less irregular than in the regime2. When Vr=14 in the regime 4, the vibration of the cylinder becomes very regular, and the displacement and lift fore is in anti-phase. This is very similar to the regime 1.

Fig.6 represents amplitude and lift force spectra of the response for some representative reduced velocities.

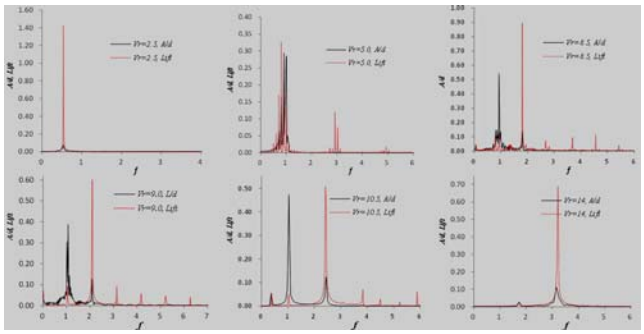

Fig.6 Amplitude and lift spectra of the response

In complex vibration, the vibration spectrum and lift force spectrum may contain multiple frequencies. The

peak frequency with the highest amplitude is defined primary frequency and the peak frequency with the second highest amplitude is called the second frequency of the vibration.

Fig.6(a) presents the vibration and lift force of Vr =2.5 in the regime 1. It can be seen that not only the amplitude but also the lift force spectra have a primary frequency. Moreover, the frequencies for vibration and lift force have the same value. In the Fig.6(b), (c), and(d), the reduced velocity is in the range of regime2, in which the amplitude has a high value. It can be seen from these figures, both the amplitude and the lift force spectra have multiple of components, and the primary or second frequency of lift force have the very approximate value with the primary frequency of the vibration. In the case of Vr=10.5 where in regime 3, the frequency of vibration contains two or three distinct components, and one of the frequency component equals to the first frequency of the lift force. When Vr=14 in the regime 4, the vibration of the cylinder contains a dominant frequency, and the primary frequency have the same value with the dominant frequency of lift force.

Fig.7 shows instantaneous vorticity contours at Vr=2.5 of the downstream cylinder.

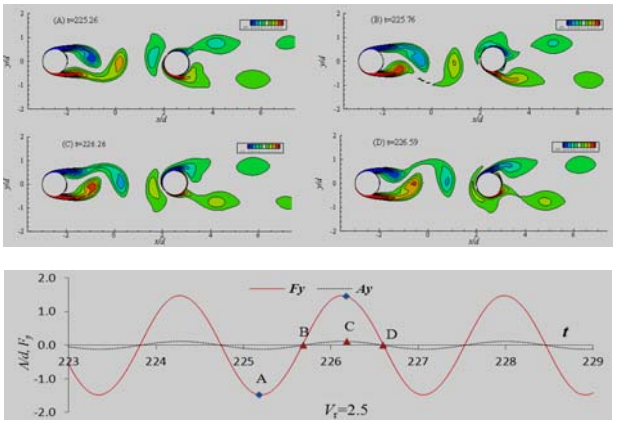

Fig.7 Instantaneous vorticity contours at V_r=2.5 of the downstream cylinder

It can be seen from Fig.7 that vortex shedding from both the top and the bottom of the upstream cylinder move to downstream close to the center line of the two cylinders. The displacement of the downstream cylinder is small and the vortex from the upstream takes little impact in the cross-direction. In one vibration period of the downstream cylinder, two single vortexes shed from the top and bottom alternately. The displacement of the vibration and the force imposing on the cylinder in the cross-flow direction are in phase.

Fig.8 shows the instantaneous vorticity contours at Vr=6.5 of the downstream cylinder, which the reduced velocity is in the regime 2.

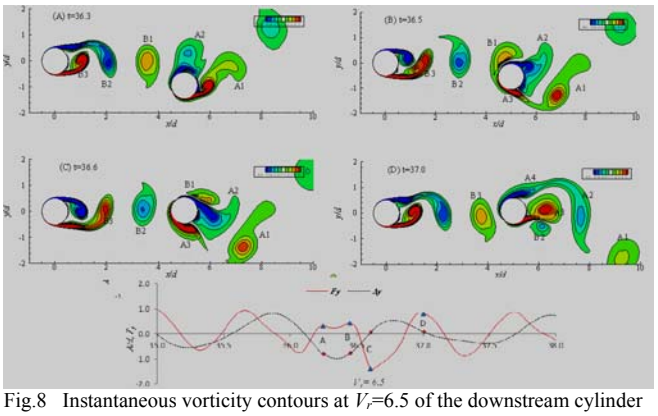

Fig.8 Instantaneous vorticity contours at V_r=6.5 of the downstream cylinder

Vr=6.5 is in the regime 2, in which the amplitudes keep in high value and the vibration spectrum combined with multiple components. At the time t=36.3 in Fig.8(a), the downstream cylinder moves to the minimum position. The positive vortex A1 is gonging to shed from the bottom of the cylinder, which imposes the maximum positive lift force to the cylinder. On the top of the cylinder, a negative vortex A2 has formed. A vortex B1 shed from upstream cylinder has close to the downstream cylinder. Vortex B2 is gonging to shed from the top of the cylinder2, and vortex B1 have formed at the bottom of the cylinder.

Fig.8(b) presents the Instantaneous vorticity contours at time of 36.5. Vortex is shedding from the downstream cylinder, and vortex A3 begin to form. The vortex A2 has moved to the downstream along the cylinder surface with its moving from down to up in the cross-direction. The vortex B3 shed from cylinder 2 reach the top of the downstream cylinder. The lift force on the cylinder begins to decrease from the positive peak value to a peak negative value. At this time vortex B2 has left the upstream cylinder and vortex B1 is going to shed.

In the Fig.8(c), the vortex A2 is shedding from the surface of the cylinder. Vortex B3 crashes the cylinder from the top and becomes weaker and weaker. The lift force gets the most negative value. When the time reaches to 37.0, the vortex B3 has dispersed, and the vortex A2 is shedding. Under the affect both the vortex A3 and vortex B2, the lift force changes from the peak of negative value to the peak of positive value.

Fig.9 shows instantaneous vorticity contours at Vr=10.5 of the downstream cylinder.

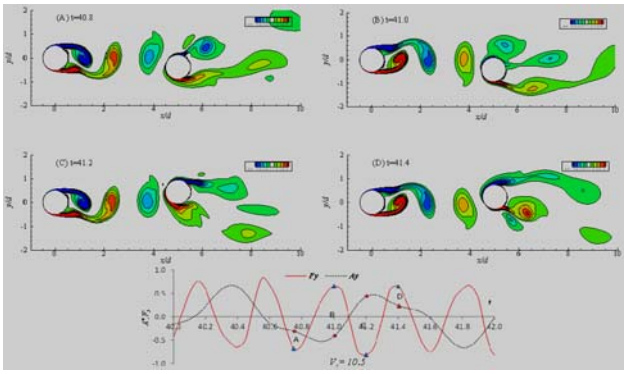

Fig.9 Instantaneous vorticity contours at V_r=10.5 of the two cylinders in tandem

It can be seen from the Fig.9, with the reducing of the vibration amplitude, the impact from the shed vortexes of the upstream cylinder become weaker and weaker.

Fig.10 represents instantaneous vorticity contours at Vr=14 of the downstream cylinder.

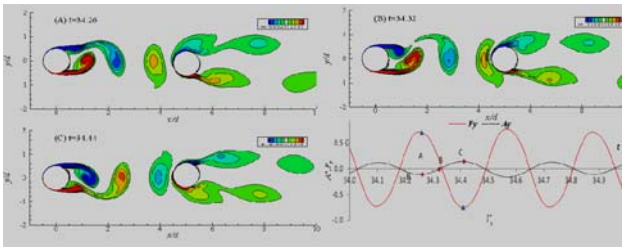

Fig.10 Instantaneous vorticity contours at V_r=14.0 of the two cylinders in tandem

Vr=14 is in the regime 4 and the amplitude is very small. The vortexes from upstream cylinder have insignificant influence on the cross vibration. The vibration of the downstream is much like the isolated cylinder.

IV. CONCLUSION

Vibration of a 1dof elastically mounted cylinder in the wake of a stationary cylinder with the same diameter was simulated numerically. N-S equations and the equation of motion are solved numerically for predicting the flow and the response of the cylinder, respectively. The mass ratio was 1.9, the U/Re was kept to a constant value of 1083. Simulations are conducted for spacing ratios of 5.5 and reduced velocities ranging from 2 to 16.5 with an interval of 0.5.

Four response regimes are found in the response of the downstream cylinder under the interference of the upstream stationary cylinder. In the regime 1 of Vr$\leq$ 4.5, the amplitude of the cylinder gradually increases with the growth of the reduced velocity, and frequency is almost increased linearly with the increasing of the reduced velocity. In the regime 2 of 5$\leq$ Vr$\leq$ 9.5, the amplitude keeps high, and the frequency is about 0.95 which near the natural frequency of the cylinder. In the regime3 of 10 $\leq$ Vr $\leq$ 12.5, the amplitude gradually decreases with the growth of the reduced velocity, and the frequency keeps lock on the natural frequency of cylinder. In the regime 2 of Vr$\geq$ 13, the amplitude keeps to very small constant value, and the frequency increases with the growth of the reduced velocity in linear manner.

In the regime 2, Vortex shedding analysis indicates the vortexes from the upstream cylinder will enhance the cross-flow direction amplitude of the downstream cylinder, and make the vibration and vortex shedding of the downstream cylinder more complex. Outside this range, the effect from the upstream stationary cylinder is small, and the vibration of the downstream cylinder is something like the isolated cylinder.

ACKNOWLEDGEMENT

The authors would like to acknowledge the National Natural Science Foundation of China (No.41476078, 41106077), and the China Spark Program (Grant No.2012GA700193, 2013GA700258), and the Open Foundation from Marine Sciences in the Most Important Subjects of Zhejiang (No.20140101), and the Scientific Research Project of Science and Technology Department of Zhejiang in China(No. 2015C33082).

REFERENCES

[1] R. E. D. Bishop and Y. Hassan, The lift and drag forces on a circular cylinder oscillating in a flowing fluid, Proc. R. Soc, (1964), England, London.
[2] C. C. Feng, The measurements of vortex-induced effects on flow past a stationary and oscillation and galloping, Master's thesis, University BC, Vancouver, Canada(1968)
[3] P. W. Bearman, Vortex shedding from oscillating bluff_bodies, Annual Review of Fluid Mechanics, 16(1984), 195-222.
[4] H. K. Williamson, Vortex dynamics in the cylinder wake, Annual Review of Fluid Mechanics, 28(1996), 477-539.
[5] B. M. Sumer and J. Fredsøe, Hydrodynamics Around Cylindrical Structures. World Scientific, Singapore(1997)
[6] C. H. K. Williamson and R. Govardhan, Vortex-induced vibrations, Annual Review of Fluid Mechanics, 36(2004), 413–455.
[7] M. M. Zdravkovich, Flow induced oscillations of two interfering circular cylinders, Journal of Sound and Vibration, 101(1985), 511-521.
[8] J. R. Meneghini, F. Saltara, C.L.R. Siqueira, and J.J.A. Ferrari, Numerical simulation of flow interference between two circular cylinders in tandem and side-by-side arrangements, Journal of Fluids and Structures, 15(2001), 327-350.
[9] J. Mizushima and N. Suehiro, Instability and transition of flow past two tandem circular cylinders. Physics of Fluids, 10(2005), 3379-3392.
[10] Y. Tasaka, S. Kon, L. Schouveiler, and P.L. Gal, Hysteretic mode exchange in the wake of two circular cylinders in tandem, Physics of Fluids, 18(2006), 084101.

[11] G.R.S. Assi, J.R. Meneghini, J.A.P. Aranha, P.W. Bearman, and E. Casaprima, Experimental investigation of flow-induced vibration interference between two circular cylinders, Journal of Fluids and Structures, 22(2006), 819-827.
[12] Z. D. Cui, M. Zhao and B. Teng, Vortex-induced vibration of two elastically coupled cylinders in side-by-side arrangement, Journal of Fluids and Structures, 44 (2014),270-291.
[13] F. R. Menter, Two-equation eddy-viscosity turbulence models for engineering applications, AIAA Journal, 32, (1994), 1598-1605.
[14] E. Guilmineau and P. Queutey, Numerical simulation of vortex-induced vibration of a circular cylinder with low mass damping in a turbulent flow, Journal of Fluids and Structures,19(2004),449-466.
[15] Z. Y. Pan, W. C. Cui, and Q. M. Miao, Numerical simulation of vortex-induced vibration of a circular cylinder at low mass-damping using RANS code, Journal of Fluids and Structures, 23,(2007), 23-37.
[16] M. Zhao, L. Cheng, B. Teng, and G. Dong, Hydrodynamic forces on dual cylinders of different diameters in steady flow, Journal of fluids and structures, 23(2007), 59-83.
[17] M. Zhao and L. Cheng, Numerical simulation of two-degree-of-freedom vortex-induced vibration of a circular cylinder close to a plane boundary, Journal of Fluids and Structures, 27, (2011),1097–1110.
[18] R. Govardhan and C. H. K. Williamson, Modes of vortex formation and frequency response of a freely vibrating cylinder, Journal of Fluid Mechanics,420,(2000),85-130.